

# A Compact Dual Band-Rejected MIMO Vivaldi Antenna for UWB Wireless Applications

Deng-Hui Li\*, Fu-Shun Zhang, Li-Xin Cao, and Yi Zhao

**Abstract**—In this paper, a novel compact dual band-rejected ultra-wideband (UWB) multiple-input multiple-output (MIMO) Vivaldi antenna is introduced and fabricated. The MIMO antenna with a small size of  $26 \times 28 \text{ mm}^2$  contains a modified ground plane and two microstrip-slot balun structures. A T-slot is etched on the ground to achieve miniaturization and high isolation, and the simulated  $|S_{11}|$  of  $-10 \text{ dB}$  impedance bandwidth is from 2.7 to 10.9 GHz. An isolation of better than 15 dB is acquired over the UWB range (3.1–10.6 GHz). Meanwhile, by introducing two split ring resonator (SRR) slits on the ground and adding two split ring resonators (SRRs) close to the microstrip-slot balun structures, dual band rejection at both WLAN (5.15–5.85 GHz) and IEEE INSAT/Super-Extended C-band (6.7–7.1 GHz) can be achieved. The MIMO antenna has high gain and very low envelop correlation coefficient (ECC  $< 0.02$ ). The measured results agree with the simulated ones, demonstrating that the UWB MIMO Vivaldi antenna is suitable for the UWB diversity applications.

## 1. INTRODUCTION

Ultra-wideband (UWB) technologies have won much attention because of some excellent advantages including high immunity to multipath interference, high-resolution capability, low cost, and high transmission rate [1]. Nevertheless, multipath fading and channel fading will bring about instability of UWB technology [2]. To solve these problems, multiple-input multiple-output (MIMO) technology which utilizes multiple antennas at both the transmitter and receiver has been proposed as an efficient method to enhance the communication quality and provide the channel capacity [3].

Many MIMO antennas which require both compact size and low mutual coupling for UWB applications have been proposed so far [4–14]. However, decreasing the size of the MIMO antenna would bring about great mutual coupling; therefore, various structures have been created to reduce the mutual coupling of MIMO antennas [4–8]. Low mutual coupling is accomplished by etching two bent slits on the ground [4], etching a narrow rectangular slot on the ground plane [5], orthogonally feeding [6, 7], spatial and polarization diversity [8]. These effective methods mentioned above can lower the mutual coupling obviously to  $-15 \text{ dB}$  or less.

However, the UWB systems from 3.1 to 10.6 GHz would bring interference to the existing narrowband communication systems like WLAN 5.15–5.85 GHz and IEEE INSAT/Super-Extended C-band (6.7–7.1 GHz). However, some antennas like [4–9] do not design band-rejected structures to stop the interference. To deal with this problem, some antennas with band-rejected function have been discussed [10–14]. In [10], two branches are added on the decoupling structure to obtain dual band-notched function. In [11, 12], by etching a pair of L-shaped slits on the ground, the rejected band at 5.5 GHz is achieved in the proposed MIMO antenna design. By introducing two split ring resonator (SRR) slots on the ground, the band-rejected function is obtained in [13]. Two strips are added between the monopole elements to create a band-notched function at 5.5 GHz in [14].

---

Received 25 June 2019, Accepted 9 August 2019, Scheduled 18 August 2019

\* Corresponding author: Deng-Hui Li (dhui\_li@163.com).

The authors are with the National Key Laboratory of Antennas and Microwave Technology, Xidian University, Xi'an 710071, China.

In this paper, a compact dual band-rejected MIMO Vivaldi antenna is proposed for UWB systems. The antenna is designed on an F4BM-2 substrate with a small size of  $26 \times 28 \text{ mm}^2$ . The isolation between two ports can be obviously improved after etching a T-slot on the ground. By employing SRR slits on the ground, the WLAN band can be rejected. Meanwhile, two SRRs are added close to the microstrip-slot balun structures to reject the IEEE INSAT/Super-Extended C-band. And the rejected mechanism is analyzed according to the surface current distributions. The measurements denote that the proposed antenna is suitable for a MIMO system.

## 2. ANTENNA GEOMETRY

The configuration of the proposed compact dual band-rejected UWB MIMO Vivaldi antenna, with a reference to Figure 1, has two symmetrical antenna elements which are fed by two symmetrical microstrip-slot balun structures. It is fabricated on a  $26 \times 28 \text{ mm}^2$  F4BM-2 substrate with a relative permittivity of 2.65 and thickness of 0.6 mm. Meanwhile, to reduce the size of the antenna and increase the isolation between Vivaldi elements, a T-slot is introduced on the ground. Furthermore, a pair of SRRs is introduced to generate the rejected band at WLAN (5.15–5.85 GHz). Two SRR slits are embedded in the ground to achieve the rejection of IEEE INSAT/Super-Extended C-band (6.7–7.1 GHz).

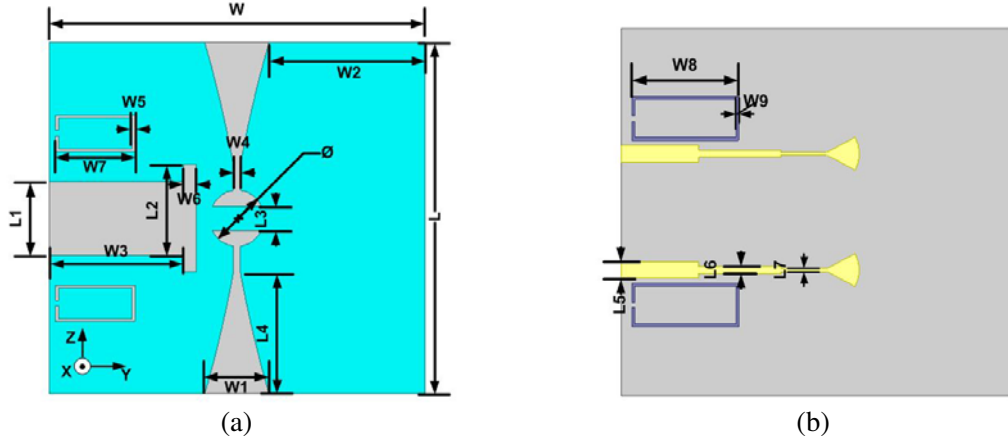


**Figure 1.** Geometry of the proposed UWB MIMO Vivaldi antenna. (a) Top view. (b) Bottom view.

The improved design values of the parameters are finally confirmed with  $W = 28 \text{ mm}$ ,  $W1 = 4.8 \text{ mm}$ ,  $W2 = 11.6 \text{ mm}$ ,  $W3 = 9.5 \text{ mm}$ ,  $W4 = 0.55 \text{ mm}$ ,  $W5 = 0.2 \text{ mm}$ ,  $W6 = 1 \text{ mm}$ ,  $W7 = 5.8 \text{ mm}$ ,  $W8 = 7.2 \text{ mm}$ ,  $W9 = 0.2 \text{ mm}$ ,  $L = 26 \text{ mm}$ ,  $L1 = 10 \text{ mm}$ ,  $L2 = 12 \text{ mm}$ ,  $L3 = 1.8 \text{ mm}$ ,  $L4 = 9 \text{ mm}$ ,  $L5 = 1.2 \text{ mm}$ ,  $L6 = 0.5 \text{ mm}$ ,  $L7 = 0.2 \text{ mm}$ . And the tapered curve function of the Vivaldi antenna is depicted as follows [15]:

$$y = \pm (c_1 e^{\alpha z} + c_2) \quad (1)$$

where  $c_1$  and  $c_2$  are determined by the opening rate  $\alpha$  and two points  $p_1(y_1, z_1)$  and  $p_2(y_2, z_2)$ .

$$c_1 = \frac{y_2 - y_1}{e^{\alpha z_2} - e^{\alpha z_1}} \quad (2)$$

$$c_2 = \frac{y_1 e^{\alpha z_2} - y_2 e^{\alpha z_1}}{e^{\alpha z_2} - e^{\alpha z_1}} \quad (3)$$

where  $p_1(y_1, z_1)$  and  $p_2(y_2, z_2)$  respectively are the bottom point and peak point of the exponential tapered curve. With the reference to Figure 1,  $y_1$  and  $y_2$  can determine  $W1$  and  $W4$ . Theoretically speaking, the cutoff wavelength of the low frequency band is twice the maximum width of the slot line, and the high frequency band of the antenna is limited by the width of the narrowest line of the slot line. Therefore,  $y_1$  and  $y_2$  can determine the low frequency and high frequency bands.  $\alpha$  means the exponential factor which can determine the beamwidth of the Vivaldi antenna, and both  $c_1$  and  $c_2$  are

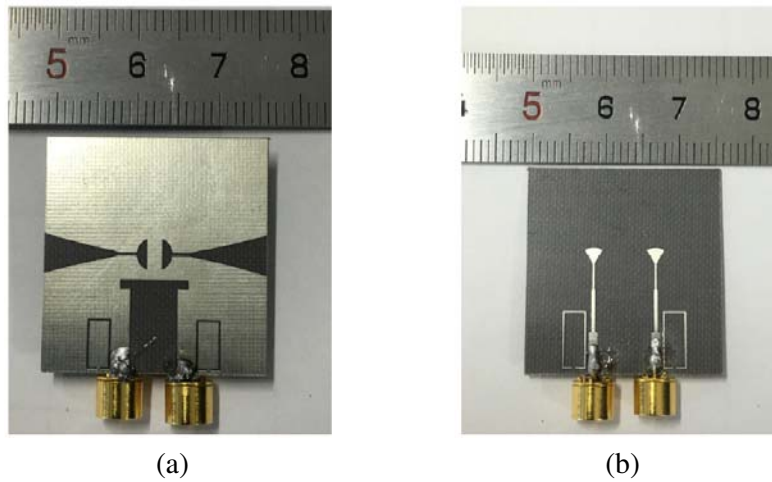


**Figure 2.** Fabricated photos of the UWB MIMO antenna. (a) Top view. (b) Bottom view.

constants. Here,  $\alpha$  is 50, and  $c_1$  and  $c_2$  can be determined by bottom point and peak point of the exponential tapered curve. So when those equations are varied, the antenna structure will change, and the characteristics of antenna will change too. Photographs of the fabricated antenna are shown in Figure 2.

### 3. ANTENNA DESIGN

The development process of the MIMO Vivaldi antenna involves three key stages: original antenna shown in Figure 3(a), improving the isolation, lowering the cutoff frequency shown in Figure 3(b), and achieving dual band-rejected function shown in Figure 3(c). Firstly, a T-slot is adopted between the two Vivaldi elements to get high isolation and lower the cutoff frequency based on the original antenna. Then, to realize the narrowband rejection at the designed notch bands over the WLAN and IEEE INSAT/Super-Extended C-band, two SRRs are added close to each microstrip feed line, and two SRR slits are embedded in the ground, respectively. The lengths of the SRR and SRR slit are 19.8 mm and 15.6 mm, respectively.

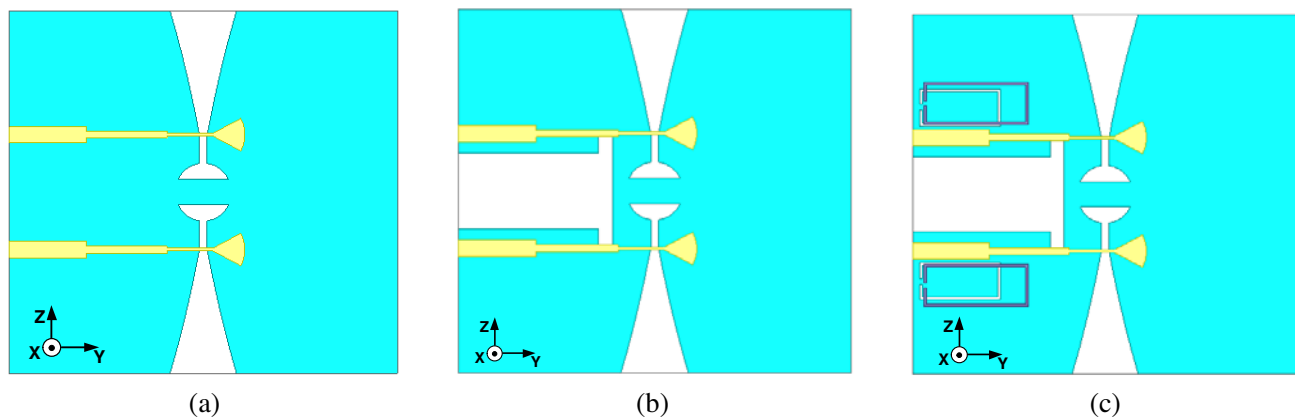


**Figure 3.** Evolution of the designed structures. (a) Antenna I. (b) Antenna II. (c) Antenna III.

### 3.1. Effects of T-Slot

#### 3.1.1. Miniaturization

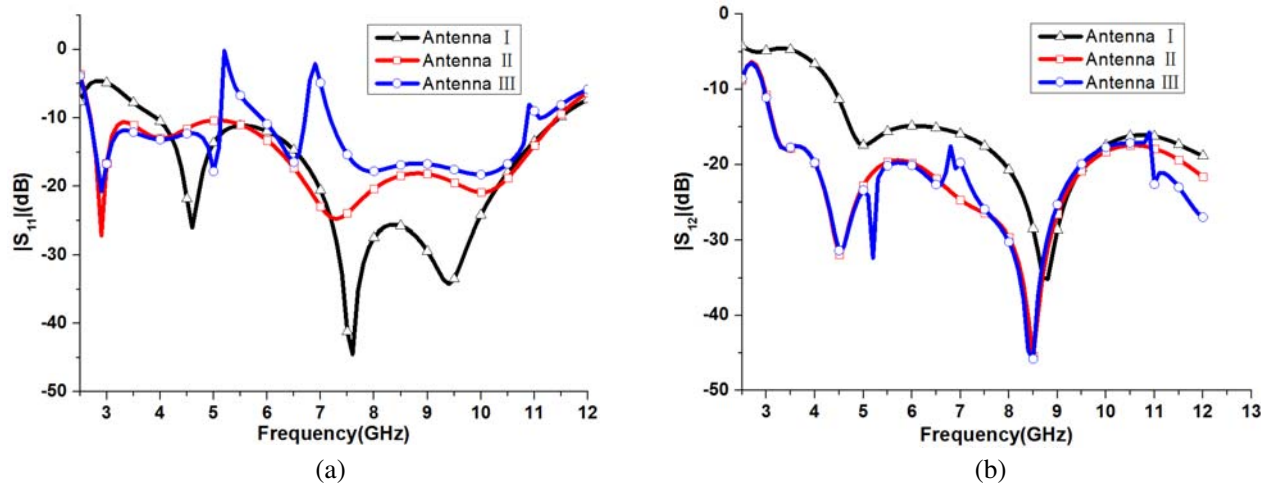
Firstly, a very distinct effect of the T-slot is to achieve miniaturization. To achieve a low cutoff frequency, the size of the antenna is always large enough which can make a long current distance to have a resonance in the low frequency band. However, compact size is necessarily required for UWB MIMO antennas, so the dimension of antenna has been an important challenge. With the reference to Figure 3(a), two Vivaldi elements are combined primordially. However, the simulated  $|S_{11}|$  is only from 3.9 to 11.5 GHz, which cannot meet the requirement of the whole UWB range. As a result, the T-slot is introduced to make a longer current distance so as to lower the low cutoff frequency, as shown in Figure 3(b).

Figure 4(a) shows the comparison of simulated  $|S_{11}|$  of the three different structures. After the improvement, it is easy to find that the method of etching a T-slot is able to miniaturize the size of MIMO Vivaldi antenna by means of lowering the minimum working frequency. So after the improvement, the simulated  $|S_{11}|$  of improved Antenna II is from 2.7 to 11.5 GHz, which meets the requirement of the UWB range.

#### 3.1.2. Improvement of the Isolation

As shown in Figure 3(a), two Vivaldi elements are simply combined with a small size of  $26 \times 28 \text{ mm}^2$ . As can be seen, a common ground is used, which can be seen as a part of the antenna radiator because of the compact dimension. The mutual coupling between the two ports will be higher due to the short distance and the existence of surface currents on the ground. Therefore, as analyzed above, we should make an improvement to lengthen the distance between the two ports. As a result, with the reference to Figure 3(b), a T-slot is introduced to obtain better isolation.

Figure 4(b) plots the simulated  $|S_{12}|$  of the three different structures. It is distinct that before etching the T-slot, the isolation between the Vivaldi elements is very low in 3-4 GHz. After the improvement,  $|S_{12}|$  of Antenna II decreases significantly from 3 to 4 GHz, indicating an increased isolation. The reason for the improved isolation is that the distance is extended by etching the T-slot between the two ports.



**Figure 4.**  $S$ -parameters of the proposed antenna. (a)  $|S_{11}|$ . (b)  $|S_{12}|$ .

### 3.2. Band-Rejected Mechanism

The WLAN band is rejected by the SRRs which are added near each microstrip-slot balun, and the IEEE INSAT/Super-Extended C-band is rejected by the two SRR slits which are etched on the ground. And the length of the SRR can determine the center of the rejected band.

### 3.2.1. Surface Current Distributions

With the reference to Figure 4(a), the impedance bandwidth of the eventually given Antenna III is 2.7–10.9 GHz with two rejected bands 5.1–5.9 GHz and 6.7–7.1 GHz. In order to understand the effect of the etched slits and SRRs in depth, Figure 5 plots the current distributions of Antenna III at the two rejected frequencies 5.5 and 6.9 GHz, respectively.

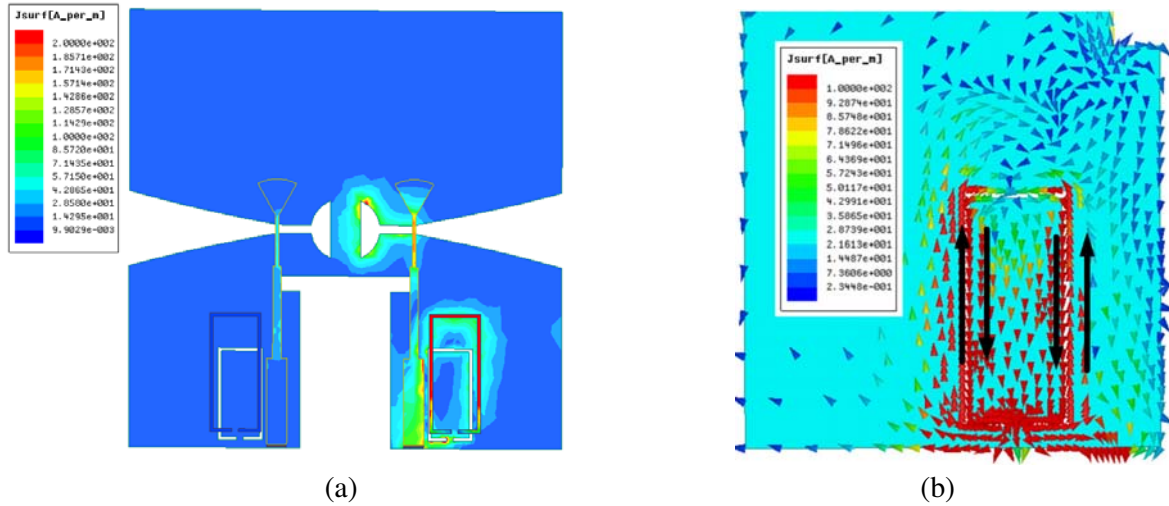


**Figure 5.** Simulated current distributions of the proposed antenna (a) 5.5 GHz. (b) 6.9 GHz.

With the reference to Figure 5(a), when operating frequency is at 5.5 GHz, the SRR can be seen as a resonator which can generate a resonance result. There is a large quantity of current energy gathering on the SRR, which impairs the radiation ability of the antenna. When operating frequency is at 6.9 GHz, with the reference to Figure 5(b), it is obvious that the currents on the two sides of the slit are in the opposite directions, and as a result, radiation from both sides will counteract in the far fields. Therefore, the current distributions demonstrate that dual-band rejection can be realized.

### 3.2.2. Parametric Study

The center of the rejected band is determined by the length of the SRR. The variation curve of  $|S_{11}|$  with different  $W7$  is displayed in Figure 6(a). It can be seen that as  $W7$  increases, the notched central frequency at the high frequency decreases gradually, while the notched central frequency at low frequency is basically unchanged. Figure 6(b) shows the variation of  $|S_{11}|$  with different  $W8$ . Similarly, as  $W8$  increases, the notched central frequency at the low frequency decreases gradually, while the notched central frequency at the high frequency is basically unchanged. Therefore, it can be seen that the notched performance of the designed antenna is mainly determined by the length of SRR. At the same time, the notched band of the designed antenna can be flexibly controlled by altering the length of the SRR.

## 4. MEASURED RESULTS AND DISCUSSIONS

To prove the simulation, a prototype of the UWB MIMO Vivaldi antenna has been finally fabricated and measured by means of a network analyzer (AV3672B). The photographs of the measurements setup are shown in Figure 7. Then  $S$ -parameters are measured. As seen from Figure 8, it can be observed that the results of the measured and simulated  $S$ -parameters have great agreement. The measured  $|S_{11}|$  is lower than  $-10$  dB from 2.7 to 10.9 GHz, which can cover the whole UWB frequency range. Besides, the measured  $|S_{12}|$  of Antenna III is lower than  $-15$  dB throughout the UWB band, representing a good isolation between the two ports.

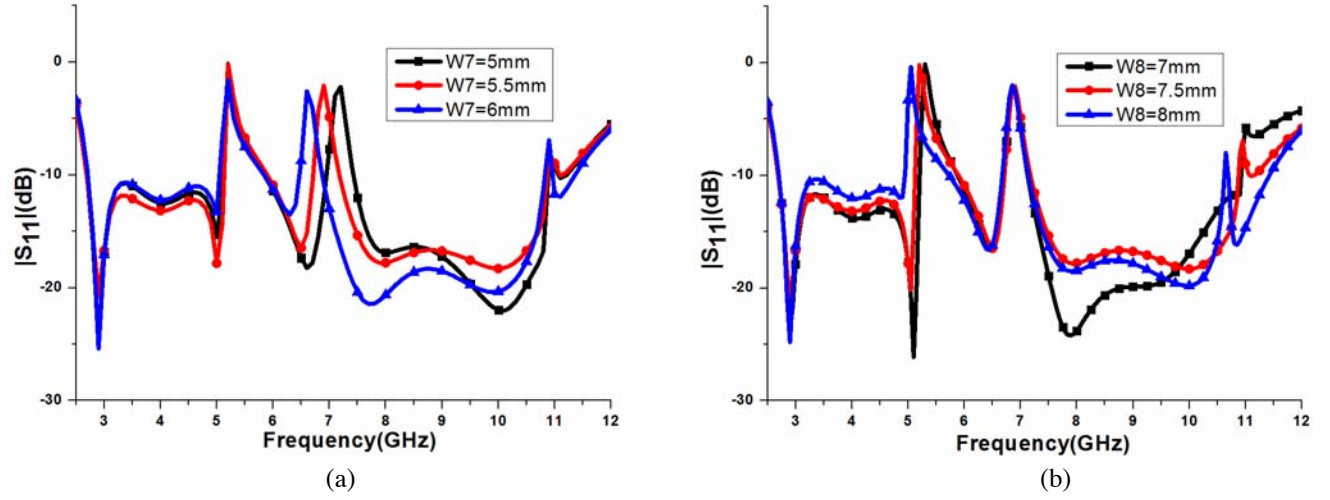


**Figure 6.** Variation curve of  $|S_{11}|$  with different  $W7$  and  $W8$  (a)  $W7$ . (b)  $W8$ .



**Figure 7.** The photos of the test equipment.

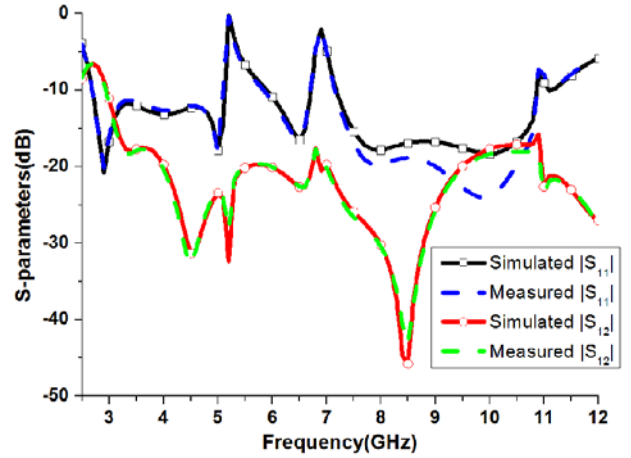


**Figure 8.** Simulated and measured  $S$ -parameters.

The key data of those reported MIMO antennas are roughly summarized in Table 1. After comparing the proposed MIMO Vivaldi antenna with the others, we can find that this proposed antenna not only insures the whole UWB frequency band but also has the smallest dimension.

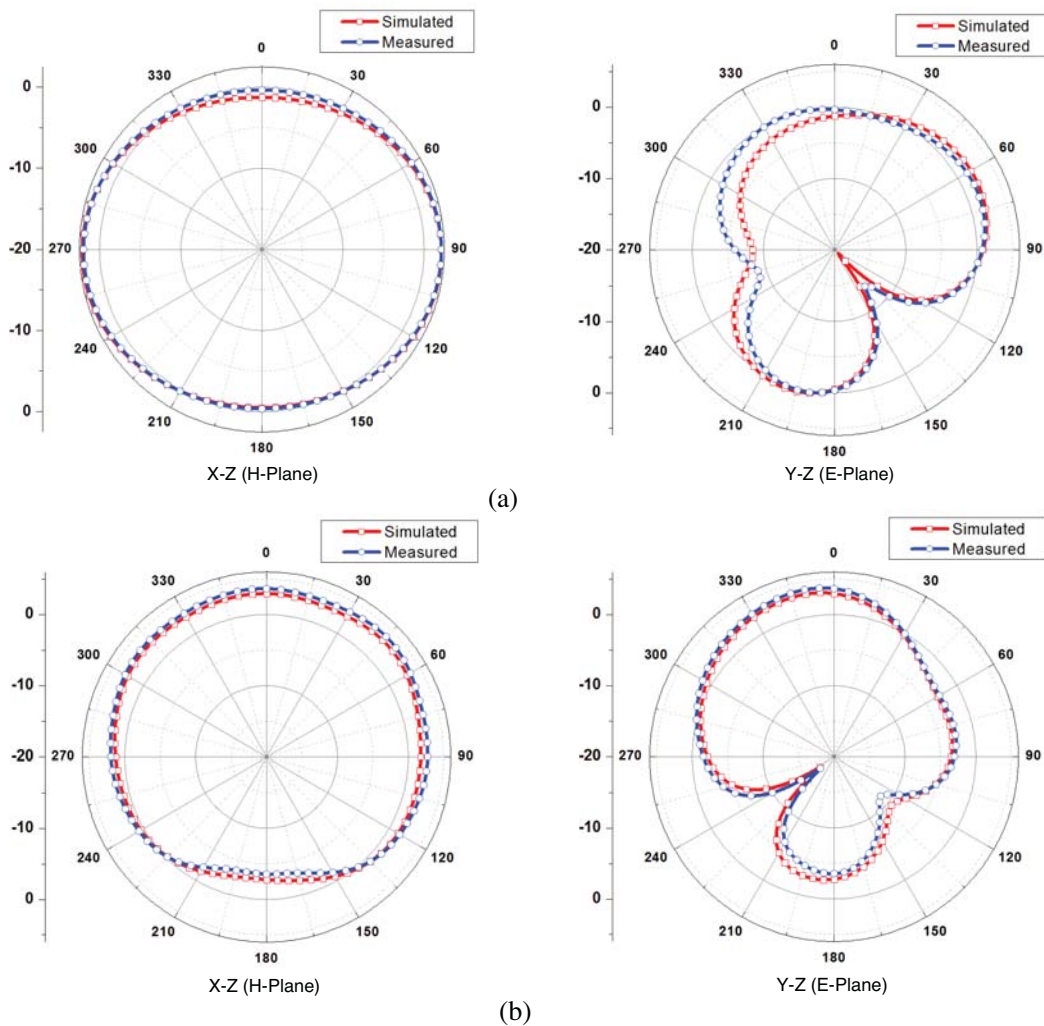
Figure 9 illustrates the measured  $E$ -plane ( $YZ$ ) and  $H$ -plane ( $XZ$ ) radiation patterns of the presented MIMO antenna at 4, 6.5, and 10 GHz, when port 1 is excited and port 2 terminated with a  $50\ \Omega$  load. It is observed that the designed MIMO Vivaldi antenna has good radiation with end-fire characteristic with the main lobe in axial direction of the tapered slot ( $z$ -direction in Figure 1) [16].

When port 1 is excited, Figure 10 plots the peak gain of the designed compact dual band-rejected MIMO Vivaldi antenna. It is observed that the peak gain of the UWB antenna without the band-rejected structures is very high, and it can be seen that the measured peak gain is from 1.6 to 6.2 dB in the whole UWB. After adding the band-rejected structures, we can find that the peak gain of the proposed antenna is very steady except the rejected bands, and the gain descends distinctly in the WLAN and IEEE INSAT/Super-Extended C-band. The simulated and measured results are in good agreement.

The envelope correlation coefficient (ECC) is an important parameter to evaluate the diversity performance of the MIMO antenna. A very low ECC means better performance of the antenna. It can

**Table 1.** Performance comparisons between the proposed antenna and the other MIMO antennas.

Reference	Size (mm <sup>2</sup> )	Impedance bandwidth (GHz)	Rejected band (GHz)	Isolation (dB)	Peak gain (dB)
[4]	78 × 40	2.40–6.55	-	18	-
[5]	32 × 32	3.10–10.60	-	15	1.7–4.2
[6]	85 × 50	2.00–9.50	-	20	-
[8]	45 × 25	3.10–11.50	-	19	0–5.5
[9]	30 × 36	3.10–10.90	-	15	3–6.9
[10]	30 × 40	3.10–10.60	3.4–3.7 & 5.15–5.35 & 5.72–5.82	15	0–4.2
[11]	38.5 × 38.5	3.08–10.80	5.03–5.97	15	1.4–3.6
[12]	36 × 36	3.10–10.60	5.15–5.825	15	2.1–6.8
[13]	48 × 48	2.50–12.00	5.1–6	15	-
[14]	22 × 36	3.10–11.0	5.15–5.85	15	1.0–5.0
proposed	26 × 28	2.70–10.90	5.1–5.9 & 6.7–7.1	15	1.6–6.2



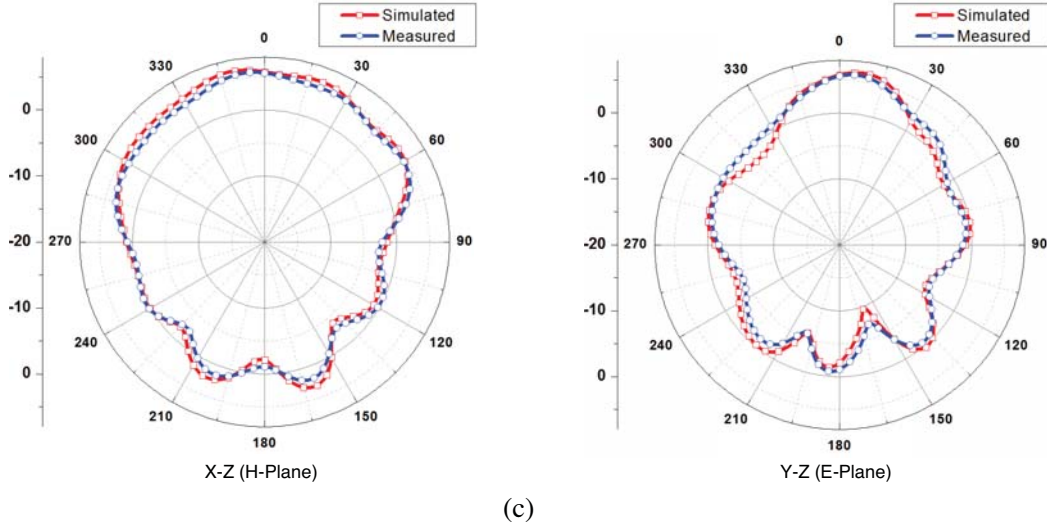


**Figure 9.** Radiation patterns of the proposed antenna (a) 4 GHz. (b) 6.5 GHz. (c) 10 GHz.

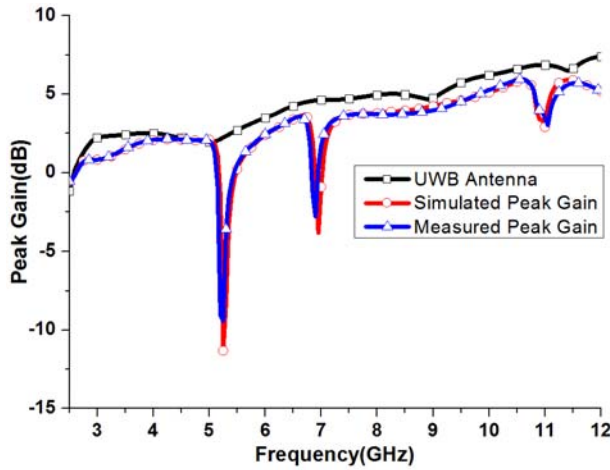


**Figure 10.** Peak gain of the proposed antenna.

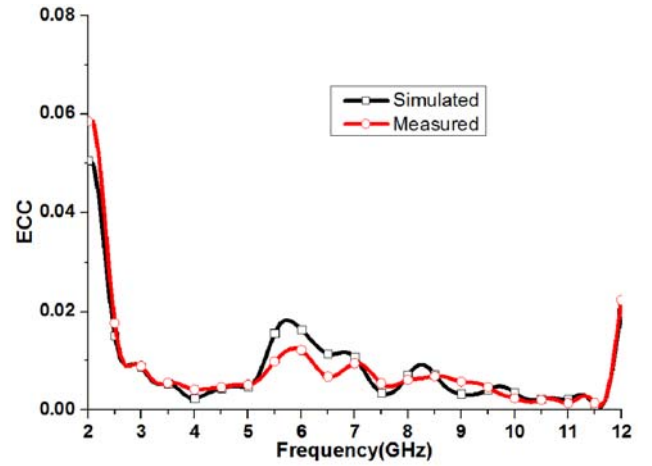


**Figure 11.** ECC of the proposed antenna.

be calculated by using the following formula [2]:

$$\text{ECC} = \frac{|S_{11}^* S_{12} + S_{21}^* S_{22}|^2}{(1 - (|S_{11}|^2 + |S_{21}|^2))(1 - (|S_{22}|^2 + |S_{12}|^2))} \quad (4)$$

With the reference to Figure 11, the simulated and measured ECCs is depicted. It is seen that the simulated and measured results are in good agreement, and a very small ECC of less than 0.02 is achieved throughout the total UWB range (3.1–10.6 GHz), demonstrating that the proposed MIMO Vivaldi antenna has good diversity characteristics.

## 5. CONCLUSION

In this letter, a compact dual band-rejected MIMO Vivaldi antenna with a small size of  $26 \times 28 \text{ mm}^2$  has been designed, measured, and analyzed for UWB applications. A T-slot is utilized between the Vivaldi elements to achieve miniaturization and improve the isolation, and the proposed antenna has an impedance bandwidth from 2.7 to 10.9 GHz, and the isolation between the two ports is improved to above 15 dB through the UWB from 3.1 to 10.6 GHz. Then two SRR slits are introduced on the ground

to generate a band rejection of the IEEE INSAT/Super-Extended C-band from 6.7 to 7.1 GHz. Adding two SRRs can achieve the other band rejection from 5.1 to 5.9 GHz of the WLAN band. The proposed antenna has very steady and high gain, small ECC, and good radiation patterns over the working band. Results prove that the MIMO Vivaldi antenna is a good candidate for UWB MIMO applications.

## REFERENCES

1. Oppermann, I., M. Hamalainen, and J. Iinatti, *UWB Theory and Applications*, Ch. 1, 3–4, Wiley, New York, NY, USA, 2004.
2. Zhao, Y., F.-S. Zhang, L.-X. Cao, and D.-H. Li, “A compact dual band-notched MIMO diversity antenna for UWB wireless applications,” *Progress In Electromagnetics Research C*, Vol. 89, 161–169, 2019.
3. Liu, X.-L., Z.-D. Wang, Y.-Z. Yin, J. Ren, and J.-J. Wu, “A compact ultrawideband MIMO antenna using QSCA for high isolation,” *IEEE Antennas Wireless Propag. Lett.*, Vol. 13, 1497–1500, 2014.
4. Li, J., Q. Chu, and T. Huang, “A compact wideband MIMO antenna with two novel bent slits,” *IEEE Trans. Antennas Propag.*, Vol. 60, No. 2, 482–489, Feb. 2012.
5. Ren, J., W. Hu, Y. Yin, and R. Fan, “Compact printed MIMO antenna for UWB applications,” *IEEE Antennas Wireless Propag. Lett.*, Vol. 13, 1517–1520, 2014.
6. Zhao, X., S. P. Yeo, and L. C. Ong, “Planar UWB MIMO antenna with pattern diversity and isolation improvement for mobile platform based on the theory of characteristic modes,” *IEEE Trans. Antennas Propag.*, Vol. 66, No. 1, 420–425, Jan. 2018.
7. Saad, A. A. R. and H. A. Mohamed, “Conceptual design of a compact four-element UWB MIMO slot antenna array,” *Microw. Antennas Propag.*, Vol. 13, No. 2, 208–215, 2019.
8. Roshna, T. K., U. Deepak, and P. Mohanan, “Compact UWB MIMO antenna for tridirectional pattern diversity characteristics,” *Microw. Antennas Propag.*, Vol. 11, No. 14, 2059–2065, 2017.
9. Zhao, H., F.-S. Zhang, and C.-Y. Wang, “A compact UWB diversity antenna,” *Int. J. Antennas Propag.*, 1–6, 2014.
10. Tang, T. and K. Lin, “An ultrawideband MIMO antenna with dual band-notched function,” *IEEE Antennas Wireless Propag. Lett.*, Vol. 13, 1076–1079, 2014.
11. Kang, L., H. Li, X. Wang, and X. Shi, “Compact offset microstrip-fed MIMO antenna for band-notched UWB applications,” *IEEE Antennas Wireless Propag. Lett.*, Vol. 14, 1754–1757, 2015.
12. Zhao, H., F.-S. Zhang, and X.-K. Zhang, “A compact band-notched Ultra-wideband spatial diversity antenna,” *Progress In Electromagnetics Research C*, 19–26, 2014.
13. Gao, P., S. He, and X. Wei, “Compact printed UWB diversity slot antenna with 5.5-GHz band-notched characteristics,” *IEEE Antennas Wireless Propag. Lett.*, Vol. 13, 376–379, 2014.
14. Liu, L., S. W. Cheung, and T. I. Yuk, “Compact MIMO antenna for portable UWB applications with band-notched characteristic,” *IEEE Trans. Antennas and Propag.*, Vol. 63, No. 5, 1917–1924, May 2015.
15. Gibson, P. J., “The vivaldi aerial,” *Proc. 9th Eur. Microw. Conf.*, 101–105, Brighton, UK, Oct. 1979.
16. Fei, P., Y. Jiao, and F. Zhang, “A miniaturized antipodal vivaldi antenna with improved radiation characteristics,” *IEEE Antennas Wireless Propag. Lett.*, Vol. 10, 127–130, 2011.